JOURNAL OF SOLID STATE CHEMISTRY 33, 219–232 (1980)

Mössbauer ^{57}Fe Spectra Exhibiting "Ferrous Character"

G. A. FATSEAS

Laboratoire de Chimie des Solides, associé au CNRS (L.A. No. 279), 2 rue de la Houssinière, (F) - 44072 Nantes Cédex, France

AND JOHN B. GOODENOUGH

Inorganic Chemistry Laboratory, South Parks Road, Oxford OX1 3QR, England

Received July 20, 1979

The term "ferrous character" reported extensively in the literature for the Mössbauer spectroscopy of octahedrally coordinated iron atoms in chalcogenides and antimonides is critically evaluated. The significance of a formal valence state for the iron is examined. The magnitude of the isomer shift is shown to provide a guide not only to the existence of high-spin versus low-spin states, but also to localized versus itinerant electrons or to extended electrons within Fe–*X*–*M* interactions (*M* = transition metal and *X* = anion). The existence of a quadrupole splitting for iron atoms in intrinsically cubic fields is only possible where the β-spin electron outside a closed α-spin half-shell is localized and Jahn–Teller coupled to lattice vibrations to form vibronic states. This situation is distinguished from quadrupolar fields associated with local-site symmetries deformed from cubic symmetry as well as from the case where the formation of itinerant β-spin electrons inhibits the formation of vibronic states.

Introduction

Mössbauer data for the halides and oxides containing nominal Fe^{2+} ions can be well interpreted by a phenomenological crystal-field theory (*1*). By analogy, Mössbauer data for octahedral-site iron atoms in chalcogenides and pnictides are said to exhibit a "ferrous character," but with important modifications that have not been adequately discussed in the literature, although it is generally recognized that "covalency" plays an important role. Table I lists Mössbauer data for some iron chalcogenides and antimonides that have been classified as exhibiting such a "ferrous character." The purpose of this note is to inquire whether the data in fact contain more precise information about the character of the "3*d*" electrons at the iron atoms.

Four features of the phenomenological crystal-field theory are of interest for the present discussion.

1. Isomer shift (IS). For high-spin ferrous ions, the IS appears to decrease systematically with increasing covalency of the metal–ligand bond. For example, the room-temperature IS for octahedral-site Fe^{2+} ions in the isostructural series FeF_2, $FeCl_2$, $FeBr_2$, and FeI_2 has the values 1.35, 1.10, 1.00, and 0.85 mm/sec, respectively (*2*).

0022-4596/80/080219-14$02.00/0

TABLE I

SOME CHALCOGENIDES AND ANTIMONIDES CONTAINING IRON WITH "FERROUS CHARACTER"

	Compound	Mössbauer data at 300 K: IS (mm/sec)	Mössbauer data at 300 K: $\|\epsilon\| = \|\Delta E_Q\|/2$ (mm/sec)	Mössbauer data at 300 K: $d\|\epsilon\|/dT$	Other properties: Structure at 300 K	Other properties: Electrica character	Other properties: Magnetic order	Other properties: T_N or T_C (K)	Other properties: Comments	Refs.
1	$Fe\|Fe_2\|S_4$	0.56	0.20		Spinel	M	Ferri[a]	606		(*40*)
2	$Fe_{1-x}Cu_x\|Cr_2\|S_4$	0.58–0.21[b]	0		Spinel	M	Ferri[c]	310 (x = 0.3) 360 (x = 0.5)	$0 < x \leq 0.7$	(*99*)
3	$Fe\|Fe_{0.06}Cr_{1.94}\|S_4$	0.60	≃0.37[d]		Spinel	M	Ferri			(*102*)
4	$Fe\|Cr_2\|S_4$	0.68	0.20	Yes	Spinel	SC	Ferri[e]	170–190	J–T distortion, $T < 10$ K	(*50–52*)
5	$Cd_{1-x}Fe_x\|Cr_2\|S_4$	0.62–0.54[f]	≃0	Yes	Spinel		Ferri[g]	90–160	$0 \leq x \leq 0.9$	(*103, 104*)
6	$Fe_{1-x}Cd_x\|Cr_2\|S_4$	0.53–0.57	0.15–0.3[h]	Yes	Spinel		Ferri	170–128	$0 \leq x \leq 0.75$	(*100*)
7	$Co\|Cr_2\|S_4$: Fe	≃0.30	≃0	Yes	Spinel		Ferri	225	A-site Fe^{2+}	(*51*)
8	$Ni\|Cr_2\|S_4$: Fe		≃0	Yes	Spinel		Ferri		A-site Fe^{2+}	(*51*)
9	$Fe\|RhCr\|S_4$	0.60	0.55		Spinel					(*105*)
10	$Fe_xCo_{1-x}\|Rh_2\|S_4$	0.55–0.57	≤0.2[n]	Yes	Spinel	SC	AF	140 (x = 0.5) 200 (x = 1)	$0.25 \leq x \leq 1$	(*105, 106*)
11	$Fe\|In_2\|S_4$	0.85–0.80[i]	1.62	Yes	Spinel	SC	AF		(IS = 0.80 mm/sec $\|31\|$)	(*31, 53*)
12	$Fe\|Cr_{2-x}In_x\|S_4$	0.77–0.85[h]	1.50		Spinel	SC	Ferri ($x \leq 0.8$) AF ($x \leq 1.3$)	75 (x = 1.0) 20 (x = 1.6) 160 (x = 0.4)	$0.2 < x \leq 2$	(*53, 86*)
13	$Fe\|Sb_2\|S_4$	0.62			Spinel	SC				(*26*)
14	$Fe\|Nb_2\|S_4$	0.77			Spinel	SC				(*26*)
15	$Fe\|Sc_2\|S_4$	0.72	≃0.10	Yes	Spinel	SC	Para		J–T distortion, $T < 10$ K	(*101*)
16	ZnS: Fe	0.65	0.30	Yes	Blende	SC	Para			(*97, 98*)
17	ZnS: Fe	0.68	0.28	Yes	Wurtzite	SC	Para			(*97, 98*)
18	CdS: Fe	0.70	0.28	Yes	Wurtzite	SC	Para			(*97, 98*)
19	$CuGaS_2$: Fe	0.75	1.39	Yes[j]	Chalcopyrite	SC	Para			(*108*)
20	$CuFe_xGe_{1-x}S_2$: Fe	0.60–0.62[h]	1.26		Chalcopyrite	SC	AF	12 (x = 0.53)	$0.5 < x < 1$	(*109*)
21	Fe_2SiS_4	0.82	1.61		Olivine		AF	125		(*78*)
22	FeS	0.7–0.83[i]	0.30		NiAs[k]	SC–M[k]	AF[k]	600	$dT_N/dP > 0$	(*57, 76, 81, 116*)
23	α-NiS: Fe	0.63	0.26		NiAs	M[l]	AF	260	1% Fe, quenched phase	(*82*)
24	$Fe_{1+x}Sb$	0.40–0.45[h]	≃0		(NiAs)[m]		AF[n]	105	$0.09 \leq x \leq 0.38$	(*70, 71, 88*)
25	Fe_2Sb_2	0.42	0.18	Yes	(NiAs)[m]	SC				(*72*)
26	$Fe_{1-x}S$	0.67	0.24		NiAs	M	AF		$0 \leq x \leq 0.08$	(*57, 116*)
27	Fe_7S_8	0.65–0.69[o]	0.11–0.32[o]		(NiAs)[p]	M	Ferri	578	"4c" superstructure	(*55, 56, 89*)
28	Fe_7Se_8	0.67–0.72[o]	0–0.20[o]	No	(NiAs)[p]	M	Ferri[q]	455	$dT_N/dP = -0.4$ deg/kbar	(*42, 58, 59, 46*)
29	Fe_3Se_4	0.59–0.62[d]	0.05–0.22	No	(NiAs)[r]	M	Ferri[s]	320	$dT_N/dP = -2.9$ deg/kbar	(*46*)[t]
30	$Fe_{0.83}Te$	0.46	0.20							(*68*)
31	Fe_3Te_4	0.40								(*69*)
32	λ-Fe_2Te_3	≃0.50	≃0.10				Pauli			(*65–67*)
33	$FeTi_2S_4$	0.78	0.22		(NiAs)[r]	M	AF	140	Fe_I, Ti_{II}	(*61, 67*)
34	$FeTi_2Se_4$	0.78	0.15		(NiAs)[r]	M	Ferro	129	Fe_I, Ti_{II}	(*54, 84*)
35	$FeTi_4S_8$	0.79	0.20		(NiAs)[r]	M	Ferro	≃50	Fe_I, Ti_{II}	(*54, 61, 91*)
36	Fe_2TiS_4	0.63	0.26		(NiAs)[r]		Ferri	285		(*60*)

37	FeV_2S_4	0.57			(NiAs)[r]	M	AF	≃130	Fe_I, V_{II}	(*62, 84*)
38	FeV_4S_8	0.89			(NiAs)[r]		Para $T > 4.2$ K		Fe_I, V_{II}	(*62*)
39	V_3S_4: Fe	0.54			(NiAs)[t]		AF	≃10	1% ^{57}Fe	(*62*)
40	$FeCr_2Se_4$	0.78	0.60		(NiAs)[r]	M		218	Fe_I, Cr_{II}	(*63*)
41	$FeNi_2Se_4$	0.65	0.17		(NiAs)[r]	M	Ferro			(*43*)
42	Fe_2NiSe_4	0.57	0.22		(NiAs)[r]	M	Ferro	67	dT_c/dP = 1 deg/kbar	(*43, 83*)
43	$FeZr_4S_8$	0.56	0.40		(NiAs)[r]		AF	15	Fe_I, Zr_{II}	(*54, 90*)
44	$Fe_{0.56}Ta_2S_4$	0.83	0.32		2H–TaS_2[u]	M	Ferro[u]	73		(*64*)
45	$FeMo_2S_4$	0.8	0.79	Yes	(NiAs)[r]		AF	101		(*73*)
46	$FePS_3$	0.87	0.76		CdI_2[r]	SC	AF	126		(*74*)
47	$FePSe_3$	0.80	0.75		CdI_2[r]	SC	AF	123		(*75*)
48	1T–$Fe_{0.1}Ta_{0.9}S_2$	0.50*	0.24		CdI_2	M		473	*IS at 480 K	(*94*)
49	FeS	0.34			Tetrag.		Para $T > 1.7$ K			(*96, 111, 112*)
50	$CuFe_2S_3$	0.72	0.20		Cubanite					(*110*)
51	Cu_2FeSnS_4	0.44	1.43		Stannite	SC				(*107*)
52	$Fe_3Ni_4S_8$	0.36	0.16		Co_9S_8		Pauli		Penthandite	(*95*)
53	M_9S_8: Fe	0.31–0.38	0.10–0.22		Co_9S_8				M = Fe, Co, Ni	(*95*)

[a] Mean magnetic moment at 4.2 K: 2.2 μ_B/mole (*40*).
[b] IS decreases linearly with x.
[c] $Cu(Cr_2)S_4$ is ferromagnetic with $\mu_{Cr} = 3\ \mu_B$ and an itinerant-electron background of antiparallel spin density $\simeq -1\ \mu_B$/mole to give a net magnetization $\simeq 5\ \mu_B$/mole (*79, 119*).
[d] Values depending on the site.
[e] Neutron-diffraction atomic moment at 4 K: $\mu_A = 4.2\ \mu_B$, $\mu_B = 2.9\ \mu_B$ (*120*). Mean magnetic moment 1.6 $_B$/mole (*119*) or 2 μ_B/mole (*79*).
[f] Reported IS = 0.60 (x = 0.22) (*104*), 0.62 (x = 0.05) (*103*), 0.54 (x = 0.9) (*103*).
[g] $Cd(Cr_2)S_4$ is a ferromagnetic semiconductor with mean magnetic moment at 4.2 K: 5.15 μ_B/mole (*121*).
[h] Values depending on x.
[i] Values depending on the author.
[j] Small T dependence.
[k] Triangular Fe_3 clustering in basal planes $T < T_\alpha = 420$ K with a semiconductor–metal transition at T_α. In the temperature range $T > T_\alpha$ spin disorder produces a maximum in the resistivity at $T = T_N$. Spins $\|c$-axis below $T_s \geq T_\alpha$; $\perp c$-axis $T_s < T < T_N$.
[l] Semimetal below first-order transition at T_N (*82*).
[m] Excess Fe in interstitial, trigonal–bipyramidal sites.
[n] Neutron diffraction atomic moment: 0.64 μ_B at 83 K (0.86 μ_B at 0 K) for single-crystal x = 0.14, and 0.88 μ_B at 10 K for polycrystalline sample = 0.10 (*88*).
[o] Values depending on the site and the author.
[p] Cation vacancies into alternate basal planes; 3c and 4c ordering within basal planes.
[q] Neutron-diffraction mean atomic moment at 296 K for 4c order: $\mu_{Fe} = 2\ \mu_B$ (*118*). Moments on both sublattices reduced from atomic values (*44*).
[r] Cation vacancies order into and within alternate basal planes; M_I in vacancy planes, M_{II} in filled planes.
[s] Neutron-diffraction atomic moments at 4.2 K: $\mu_{Fe_I} = 3.25\ \mu_B$, $\mu_{Fe_{II}} = 1.94\ \mu_B$ (*85*).
[t] Fe_3Se_4 was reported, from Mössbauer data, to have iron atoms with two different electronic states, Fe^{2+} and Fe^{3+} (*77*). We have, however, found (*43*), by studying this compound (and also two other isostructural Fe_2TiSe_4, Fe_2NiSe_4), that their Mössbauer spectra are perfectly fitted by only one, practically, IS for all sites, in agreement with other metallic NiAs phases, like Fe_7Se_8 and $FeTi_2S_4$.
[u] Fe atoms intercalated between TaS_2 layers. Mean atomic moment per Fe atom at 4.2 K: 3.5 μ_B (*64*).

Within the crystal-field theory (*3*), covalent mixing does not change the symmetry properties of the $3d$ electrons so long as they remain localized; but it does extend the wave functions out over the nearest-neighbor anions to lower the intraatomic electrostatic interactions between the $3d$ electrons and to introduce interatomic Fe–X–Fe interactions. In addition, covalent mixing is not the same for crystalline $3d$ orbitals of different symmetry, which is the major cause for reduction of the fivefold atomic-orbital degeneracy of a free-ion D state. In a cubic crystalline field, an orbitally fivefold-degenerate, free-ion D state is split into an orbitally threefold-degenerate T_2 state and a two-fold-degenerate E state. A free Fe^{2+} ion is in a high-spin ^5D: $d_\alpha{}^5 d_\beta{}^1$ state, where the subscript α refers to the majority-spin state and β to the minority-spin state on the atom. In a cubic octahedral interstice, the ^5D ground state of an Fe^{2+} ion becomes $^5T_{2g}$: $t_{2\alpha}{}^3 e_\alpha{}^2 t_{2\beta}{}^1$; in a cubic tetrahedral site it is ^5E: $e_\alpha{}^2 t_{2\alpha}{}^3 e_\beta{}^1$. In an octahedral site, the e orbitals σ-bond with nearest-neighbor ligands; in a tetrahedral site the t_2 orbitals do. The cubic-field splitting of t_2 and e orbitals of the same spin is Δ_c; the intraatomic-exchange splitting of states of different spin is Δ_{ex}. The cation $3d$ covalent mixing with ligand orbitals increases Δ_c and decreases Δ_{ex}; if it is strong enough to make $\Delta_c > \Delta_{ex}$, the high-spin configuration is no longer stable. For an octahedral-site Fe^{2+} ion, the high-spin $^5T_{2g}$ state becomes unstable relative to a low-spin $^1A_{1g}$: $t_{2\alpha}{}^3 t_{2\beta}{}^3$ state, which is diamagnetic. In the $^1A_{1g}$ state, covalent mixing into the empty e orbitals is particularly strong, and the IS is reduced to a value <0.5 mm/sec relative to elemental iron.

Where Fe–X–Fe interactions are present, the conditions for localization of the "$3d$" electrons break down if the interatomic interactions become stronger than the intraatomic interactions (*3*). Since covalent mixing increases the Fe–X–Fe interactions and decreases the intraatomic interactions, strong covalent mixing may induce a transition from localized to itinerant electrons; for electrons of the same spin, itinerant character is more probable if they occupy σ-bonding rather than π-bonding orbitals. We designate itinerant "$3d$" electrons in σ-bonding and π-bonding orbitals with the labels σ^* and π^* because the localized-electron symmetries are maintained only at the center of the Brillouin zone in itinerant-electron band theory. At a high-spin Fe^{2+} ion, the majority-spin electrons experience a maximum intraatomic-exchange stabilization whereas the single minority-spin electron has none. Therefore, at a high-spin Fe^{2+} ion the minority-spin electron in a π-bonding orbital may become delocalized before a majority-spin electron in a σ-bonding orbital. A breakdown of $3d$-electron localization is commonly found in oxides containing transition-metal cations of higher formal valence state; in particular, it occurs where the energy of the ground "$3d$"-electron manifold is overlapped by the O^{2-}: $2p^6$ bands. This latter condition is fulfilled in chalcogenides containing transition-metal cations of lower formal valence state; it may be found—especially for the minority-spin electron—in chalcogenides containing Fe^{2+} ions, as is discussed below. In oxides, the critical condition for formation of σ^* band states is generally similar to that for formation of a low-spin state; for larger anions, where covalent mixing reduces more rapidly the intraatomic electrostatic energies and the difference between π-bond and σ-bond covalency is smaller, the formation of itinerant-electron σ^* states within a high-spin configuration is more probable. Since the IS is a measure of the reduction in the intraatomic electrostatic energies due to covalent mixing, an IS <0.8 mm/sec may be associated with itinerant-electron σ^* electrons in a high-spin configuration where there are Fe–X–Fe interactions. Where there are

only Fe–*X*–*X*–Fe or Fe–*X*–*M*–*X*–Fe interatomic interactions, which are weaker than Fe–*X*–Fe interactions, localized-electron high-spin configurations may exist to a lower IS value; but in any case an IS <0.5 mm/sec probably signals a low-spin configuration.

2. *Quadrupole splitting* (*QS*). Deformation of an octahedral or tetrahedral site from cubic to a lower symmetry introduces a quadrupolar crystalline field. The quadrupole splitting (QS) of the Mössbauer spectrum, defined as $\Delta E_Q = 2\epsilon$, is a measure of the electric-field gradient at the nucleus:

$$V_{ij} = V_{ij}(\text{val}) + (1 - \gamma_\infty)V_{ij}(\text{lat}),$$

where $(1 - \gamma_\infty) \simeq 10$ (*4*). The two contributions to V_{ij} represent a valence-electron term, responsible for a ΔE_0, and a lattice term ΔE_l of opposite sign:

$$\Delta E_Q = \Delta E_0 - \Delta E_l.$$

Within crystal-field theory (*3*), a high-spin Fe^{2+} ion has a single β-spin electron occupying, in a cubic field, an orbitally degenerate $^5T_2$ or ^5E ground state. Although the orbital angular momentum is quenched (to first order) in the ^5E ground state for tetrahedral coordination, the accidental degeneracy may be removed by coupling to lattice vibrational modes of E symmetry. This coupling is possible because the electron configuration can be rearranged in a time short compared to the period of a lattice vibrational mode. In the absence of a static deformation of the interstice, the Jahn–Teller coupling produces vibronic states that are split; the electron configuration of a vibronic state introduces an important electronic component ΔE_0 to the QS even though the average lattice symmetry remains cubic. The orbital angular momentum of an octahedral-site $^5T_{2g}$ ground state is not completely quenched in first-order theory, and spin–orbit multiplet splitting couples to the Jahn–Teller splitting of the ground state. Above the magnetic-ordering temperature, thermal disordering of the spins may produce a time-averaged cubic symmetry, but anisotropic vibrations can produce a QS.

It is important to note that such a theory is only applicable if the β-spin electron of the high-spin configuration is localized. Formation of itinerant β-spin electrons remove the orbital degeneracy of the ground state by producing a band of itinerant-electron states. In this case, there is no accidental degeneracy to be removed by the formation of vibronic states, and any ΔE_Q should be associated with a static ΔE_l introduced by the intrinsic crystallographic symmetry.

The magnitude of the ΔE_Q introduced by Jahn–Teller splitting of vibronic states is estimated to be about 5 mm/sec for free-atom wavefunctions (*5*). In a real crystal, this value is reduced by a factor κ^2, where the positive fraction κ is smaller the greater the π-bond covalent mixing of the β-spin orbital with nearest-neighbor ligands. In solids, where the β-spin orbitals are definitely localized, a $|\Delta E_Q| = |2\epsilon| > 3$ mm/sec is commonly observed at room temperature (*2*). In the absence of Fe–Fe or Fe–*X*–Fe interactions, a covalent mixing strong enough to suppress significantly the Jahn–Teller vibronic coupling may yet leave the β-spin electrons localized (in the crystal-field sense); in this case, a ΔE_Q may still be associated with a crystallographically cubic site, but its magnitude can be quite small.

3. *Temperature-dependent QS*. The vibronic splittings of cubic-field degeneracies are small enough for appreciable population of the excited states at higher thermal energies, kT. Therefore, a $d|\Delta E_Q|/dT < 0$ is a characteristic feature of high-spin ferrous compounds and complexes containing localized $3d^6$ manifolds in time-averaged cubic symmetry (*6–31*). However, this characteristic should no longer manifest itself if the β-spin electrons have been rendered

itinerant as a result of Fe–Fe or Fe–X–Fe interactions.

In the presence of a static quadrupolar field, the cubic-field electronic degeneracies are lifted by normal crystal-field considerations. Static distortions may induce large enough splittings of the electronic energy levels to eliminate any temperature dependence of the QS that is not reflected in the magnitude of the local-site deformation. Where static deformations reflect a cooperative Jahn–Teller coupling, these deformations may have a strong temperature dependence just below the transition temperature at which the cooperative deformations appear, particularly if the transition is second order. In this latter case, a temperature-dependent QS should persist above the transition temperature because of dynamic Jahn–Teller coupling. Where static deformations are due to the intrinsic symmetry of the structure, the lattice quadrupolar field would have a marked temperature dependence only in crystals having an anisotropic thermal expansion.

4. Linear IS/QS correlations. A linear IS/QS correlation has been found for a few isostructural series of ferrous compounds (*32–34*), and it has been suggested that this correlation should extend to more covalent crystals. However, we must anticipate a limited applicability for this observation. In particular, it should not apply where the β-spin electrons are delocalized. The IS is primarily influenced by σ-bond covalency whereas the QS of high-spin Fe^{2+} ions relects the π-bonding β-spin configuration. Where the β-spin electrons are delocalized, the QS should be due to static deformations alone; static deformations induced by the intrinsic crystal symmetry would be relatively independent of the covalent mixing responsible for modulating the IS.

Extrapolation from Iron Sulfides

1. Formal valence. In the oxides and halides, a localized $Fe^{2+}: 3d^6$ level generally lies within an energy gap between empty conduction and filled valence bands. Removal of an electron produces a localized $Fe^{3+}: 3d^5$ configuration at an energy about 3 eV below the $Fe^{2+}: 3d^6$ level (*3, 35*).

In sulfides the $Fe^{2+}: 3d^6$ level lies near the top of the $S^{2-}: 3p^6$ valence bands (*36*). In fact, a tetrahedral-site $Fe^{2+}: 3d^6$ level lies discretely above the top of the valence bands whereas the corresponding octahedral-site level is overlapped by the $S^{2-}: 3p^6$ valence bands. Therefore, an $Fe^{3+}: 3d^5$ configuration is a meaningful formal valence state for a tetrahedral-site iron atom, as is well known in chalcopyrite, $CuFeS_2$. However, an $Fe^{3+}: 3d^5$ configuration is not possible for octahedral-site iron in sulfides. Any attempt to oxidize an octahedral-site Fe^{2+} ion to the Fe^{3+} state creates holes in the $S^{2-}: 3p^6$ valence bands, which is why Fe_2S_3 is unstable relative to the disproportionation products $FeS + FeS_2$. In FeS_2, the valence-band holes are ordered into the antibonding $3p$ states of complex $(S_2)^{2-}$ ions, and the iron has the formal valence state $Fe^{2+}: 3d^6$.

The valence bands of the selenides, tellurides, and antimonides are even less stable than the $S^{2-}: 3p^6$ bands, so the octahedral-site $Fe^{2+}: 3d^6$ level lies even further below the top of the valence bands in these compounds. However, in all these compounds we should anticipate that, if there is no complex-anion formation, molar concentrations of holes lower the Fermi energy into the $Fe^{2+}: 3d^6$ level (or narrow band) to create cation-d as well as anion-p holes. Although the Mössbauer spectrum may exhibit a "ferrous character," assignment of a formal valence state to the iron atoms is not meaningful.

2. Delocalization of 3d electrons. Where the valence bands overlap the $3d^n$ manifold in oxides, delocalization of the $3d$ electrons is commonly found (*3*). Therefore, we may

anticipate at least a tendency toward delocalization of the $3d$ electrons in ferrous chalcogenides and antimonides wherever Fe–Fe interactions and/or Fe–X–Fe interactions occur. In fact, high-spin iron ions in edge-shared (or face-shared) octahedra or tetrahedra are associated with structural and transport properties indicative of itinerant β-spin electrons (*36*). Therefore, we may assume that high-spin iron atoms in chalcogenides and antimonides have itinerant β-spin electrons wherever Fe–Fe interactions occur across shared octahedral-site or tetrahedral-site edges and faces.

Delocalization of σ-bonding electrons via Fe–X–Fe interactions is less directly manifest if the orbitals are half-filled, as is the case for high-spin Fe^{2+} or Fe^{3+} ions. At lower temperatures, antiferromagnetic ordering of any spontaneous atomic moments is stabilized, and the spin densities of antiferromagnetically coupled σ^* electrons tend to be paired. As a result, any spontaneous atomic moments associated with antiferromagnetically coupled σ^* electrons are sharply reduced from the free-atom moments (*3*). The magnitude of the atomic moments depends on the relative strength of the interatomic and intraatomic interactions. Where the ratio of interatomic/intraatomic interactions is large enough, spontaneous magnetism is suppressed; in this case metallic samples exhibit only a weak, temperature-independent Pauli paramagnetism. A distinguishing feature for itinerant versus localized antiferromagnetism is the pressure dependence of the magnetic-ordering temperature T_N: a $dT_N/dP < 0$ is found for itinerant-electron antiferromagnetism and a $dT_N/dP > 0$ for localized-electron antiferromagnetism (*3*).

Discussion

Application of these ideas to the data of Table I is instructive.

The first group of compounds all have the cubic spinel structure containing tetrahedral (A) cations (outside brackets in structural formula, Table I) and octahedral (B) cations. The intrinsic symmetry at a tetrahedral site is cubic, so any ΔE_Q from A-site Fe^{2+} ions is associated with localized β-spin electrons and should exhibit a $d|\epsilon|/dT < 0$. The octahedral sites, on the other hand, have a trigonal axial field; its magnitude is modulated by the anion-position parameter u. Therefore, Mössbauer resonances from B-site atoms will generally exhibit a ΔE_Q. The temperature dependence of ΔE_Q, $d|\epsilon|/dT$, will reflect that of the u parameter, which would normally be small, and any contribution from Jahn–Teller vibronic states associated with localized minority-spin electrons at Fe^{2+} ions.

If Fe^{2+} and Fe^{3+} ions coexist in high concentration on tetrahedal sites of chalcogenide spinels, electron transfer from an Fe^{2+} to an Fe^{3+} ion does not require an activation energy, and in this sense at least the minority-spin electrons become itinerant. Therefore the mixed-valency condition is sufficient to suppress any localized-electron vibronic states at high-spin ions, and hence any QS of A-site-iron Mössbauer resonances.

In the case of B-site iron, nearest-neighbor Fe–Fe interactions are strong enough to delocalize the minority-spin electrons at Fe^{2+} ions even without mixed valency. Any mixed Fe^{2+}, Fe^{3+} valency of B-site ions is complicated by the presence of holes in the S^{2-}: $3p^6$ bands; but the presence of broad-band holes only enhances delocalization of the minority-spin electrons. Therefore, only for low concentrations of B-site Fe^{2+} ions can we expect to find localized minority-spin electrons at B-site iron.

Among the spinels listed in Table I, the tetrahedral-site iron atoms are all Fe^{2+} ions except in three cases: Fe_3S_4 = $Fe[Fe_2]S_4$, $Fe[_{0.06}Cr_{1.94}]S_4$, and $Fe_{1-x}Cu_x[Cr_2]S_4$. Therefore all but these three should have localized β-spin electrons at

the tetrahedral iron and a corresponding QS having a $d|\epsilon|/dT < 0$. Where quadrupole data are available, exclusive of these exceptions, the temperature dependence is normal, as anticipated. For $Fe[In_2]S_4$, the magnitude of $\Delta E_Q = 2\epsilon$ is also characteristic of localized electrons; in $Fe[Cr_2]S_4$ it is greatly reduced. Such a reduction indicates a π-bond covalent contribution to the e_β orbital that is strong enough to weaken appreciably the vibronic coupling. In fact, $Fe[Cr_2]S_4$ exhibits a static Jahn–Teller distortion only below 13 K (*37, 38*); in the corresponding oxide it sets in below 135 K (*39*).

Independent evidence for strong covalent mixing comes from the small room-temperature IS; in $Fe[Cr_2]S_4$ it is only 0.68 mm/sec relative to that of elemental iron. Such a small IS is expected to be associated with Fe–*X*–Fe interactions that are strong enough to produce itinerant σ^* electrons. However, if *M* is not Fe in $Fe[M_2]S_4$, the interactions via a single anion are Fe–*X*–*M* interactions, and the relative energy levels on these unlike cations concentrate the σ^*-electron charge density on the iron atoms. This interpretation of the low IS implies that in Fe_3S_4, where Fe–*X*–Fe interactions are encountered, the spontaneous atomic moments measured by low-temperature neutron diffraction should be sharply reduced.

In sulfides, the minority-spin energies of tetrahedral-site iron generally lie above the broad $S^{2-}: 2p^6$ bands; the corresponding states at octahedral-site iron have lower energies (*36*). Moreover, octahedral chromium has its d^3 configuration at an energy below the top of the $S^{2-}: 2p^6$ bands and a high-spin d^4 configuration at a higher energy than the tetrahedral $Fe^{2+}: d^6$ configuration. Therefore, $Fe[Fe_2]S_4$ has only Fe^{3+} ions on tetrahedral sites and $Fe[Fe_{0.06}Cr_{1.94}]S_4$ has 0.06 holes per formula unit in the tetrahedral minority-spin bands, which makes these electrons itinerant. In neither case can we expect a QS from the tetrahedral iron; the QS is to be associated with the intrinsic axial field at the octahedral-site iron. If the minority-spin electrons on the *B*-site ions are delocalized, as is the case in Fe_3S_4, any temperature dependence of the QS should be reflected in that of the S^{2-}-ion *u* parameter. The low isomer shift (IS = 0.56 mm/sec) in Fe_3S_4 reflects a higher average formal valence on the iron atoms, which increases the Fe–S covalent mixing. Magnetic data (*40*) reveal the reduced atomic moments anticipated for high-spin iron with itinerant σ^* electrons; apparently the Fe(tet)–S–Fe(oct) interactions are strong enough to produce itinerant σ^* electrons, but not quite strong enough to overcome the strong correlations and produce a low-spin state.

The $Cu^+: 3d^{10}$ configuration overlaps the $S^{2-}: 3p^6$ bands in most sulfides, which perturbs these broad bands. The proportion of Cu : 3*d* and S : 3*p* character at the top of the broad valence bands is not known. The system $Fe_{1-x}Cu_x[Cr_2]S_4$ contains one hole per copper atom in the minority-spin band of the iron atoms over the range $0 < x < 0.5$, and no *A*-site QS is anticipated because these holes are itinerant. For > 0.5, $(2x - 1)$ holes per formula unit occupy the broad valence bands. Broad-band holes render the system metallic, and the end member $Cu[Cr_2]S_4$ is a metallic ferromagnet. Antiparallel coupling of the iron moments to the *B*-site chromium moments makes ferrimagnetic the system $Fe_{1-x}Cu_x[Cr_2]S_4$, $0 < x \leq 0.7$.

In the second group of sulfides in Table I, substitution of a small concentration of Fe^{2+} ions for tetrahedrally coordinated Zn^{2+} or Cd^{2+} in ZnS : Fe and CdS : Fe introduces isolated, tetrahedrally coordinated Fe^{2+} ions having localized β-spin electrons. The sites are intrinsically cubic, so any QS is due to Jahn–Teller vibronic states and should exhibit a $d|\epsilon|/dT < 0$, which is what has been observed. In the chalcopyrite

$CuGaS_2$ ordering of Cu^+ and Ga^{3+} ions makes the structure tetragonal and imposes an intrinsic axial field on the tetrahedral sites. Substitution of a small concentration of Fe^{2+} ions for $(Cu^+ + Ga^{3+})$ ions produces a Mössbauer spectrum having a QS containing both a lattice contribution and a vibronic contribution. The latter dominate the temperature dependence of $|\Delta E_Q|$ to give a normal $d|\epsilon|/dT < 0$. Similarly, an intrinsic axial field is present in the chalcopyrite system $CuFe_xGe_{1-x}S_2 = Cu^+Fe_{2y}{}^{3+}Fe^{2+}_{0.5-y}Ge^{4+}_{0.5-y}S_2{}^{2-}$. For small values of y, the concentration if iron atoms may be small enough for the β-spin electrons to remain localized, at least in the paramagnetic temperature range $T > T_N$. Correlation of $d|\epsilon|/dT$ with the transport properties as a function of y in this system would be instructive. The olivine structure of Fe_2SiS_4 contains a close-packed hexagonal anion array with Si occupying one-eighth of the tetrahedral sites; the Fe^{2+} ions occupy alternate basal planes of close-packed octahedra sharing common edges. Therefore the iron atoms experience an intrinsic axial field that is primarily responsible for the QS.

In the third group of compounds listed in Table I, high-temperature FeS and α-NiS have the $B8_1$ structure of NiAs. This structure consists of a close-packed-hexagonal anion array with cations occupying all the octahedral sites, which form a simple-hexagonal array. The octahedral sites share common edges with basal-plane near neighbors and common faces with c-axis near neighbors. Below $T_\alpha = 420$ K, FeS is distorted by the formation of triangular Fe_3 clusters within the basal planes. The compound is semiconducting at temperatures $T < T_\alpha$, metallic in the range $T > T_\alpha$. A maximum in the resistivity vs temperature curve at T_N is due to spin-disorder scattering; it does not indicate semiconductor behavior in the range $T_\alpha < T < T_N$. These data indicate that the β-spin electrons in FeS are itinerant, so the QS is due to the trigonal component of the crystalline field at $T > T_\alpha$, the biaxial components at $T < T_\alpha$. Any temperature variation in ΔE_Q should be reflected in the crystal structure. A similar situation should apply to the tetragonal form of FeS (last group in Table I), which seems to contain itinerant $3d$ electrons (*36*).

The stable room-temperature form of NiS is millerite, but the metastable α-NiS form can be obtained at room temperature and below by rapid quenching. The onset of magnetic order at T_N is associated with a first-order dilatation of the hexagonal lattice, indicative of itinerant $3d$ electrons that become more strongly correlated at temperatures $T < T_N$. Substitution of small concentrations of Fe^{2+} for Ni^{2+} ions have been made, and the observed QS reflects at least the trigonal component of the crystal field. Investigation of the temperature dependence of ΔE_Q would indicate whether the iron β-spin electrons are localized.

The antimonides $Fe_{1+x}Sb$ have the excess iron randomly distributed in interstitial trigonal–bipyramid sites of the $B8_1$ structure. Mobile holes in the Sb : $4p^6$ and Fe : d^6 bands are itinerant, and any QS must have a $d|\epsilon|/dT$ that reflects changes in the c/a ratio. The $d|\epsilon|/dT < 0$ reported for semiconducting Fe_3Sb_2, which has filled Sb: $4p^6$ and Fe: d^6 bands, should also reflect changes in the c/a ratio since the $3d$ electrons are expected to be itinerant in so covalent a compound.

With the exception of cubic Fe_3S_4, the iron chalcogenides $Fe_{1-x}X$ (where X = S, Se, Te and $0 < x \leq 0.25$) crystallize with a hexagonal-close-packed anion array having its simple-hexagonal array of octahedral sites nearly filled with iron atoms. The $B8_1$ structure of NiAs has the octahedral sites filled ($x = 0$). In Fe_7X_8 and Fe_3X_4, the cation vacancies order into alternate basal planes of the simple-hexagonal array; at lower temperatures they may order within

these planes. Two holes per cation vacancy are introduced into the overlapping S^{2-} : $2p^6$ and Fe^{2+} : $3d^6$ bands. For small x, the holes may be confined to the top of the valence band, but for larger x they are shared between valence p^6 bands and Fe^{2+}: d_β bands. Under these "mixed-valency" conditions, the β-spin electrons are itinerant, and any temperature dependence of $\Delta E_Q = 2\epsilon$ should be mirrored in the crystallographic axial ratio c/a, which modulates an intrinsic axial-field component. In the absence of an anisotropic thermal expansion, the QS should be relatively independent of temperature, as has been noted for Fe_7Se_8 and Fe_3Se_4 (*41–43*). The small isomer shifts for all these iron chalcogenides implies itinerant, though strongly correlated, σ^* electrons. The iron tellurides, with IS $\lesssim$ 0.5 mm/sec, appear to be in a low-spin state without any spontaneous magnetism. Single-crystal neutron-diffraction data for Fe_7Se_8 has been interpreted on the basis of a high-spin state with a reduced magnetic moment for all the iron atoms (*44*). The electronic specific heat and transport properties are consistent with a high density of states at the Fermi energy (*45*), indicating that E_F lies within a narrow Fe^{2+}: $3d^6$ band; and a $dT_N/dP < 0$ provides independent evidence for itinerant-electron antiferromagnetism (*46*); i.e., for itinerant, though strongly correlated, σ^* electrons.

The ferromagnetic, metallic compounds $FeNi_2Se_4$ and Fe_2NiSe_4 also have isomer shifts characteristic of itinerant $3d$ electrons. In these compounds, a large concentration of holes exists in overlapping Se : $4p^6$ and Fe : d^6 bands, and any $d|\epsilon|/dT$ should be reflected in temperature variations of the c/a ratio of the hexagonal structure. The compounds $FeCr_2Se_4$ and $FeMo_2S_4$, on the other hand, contain Fe^{2+} and Cr^{3+} or Mo^{3+} ions ordered into alternate basal planes of $B8_1$ structure. With only half the sites of an iron layer occupied, the possibility exists of localized β-spin electrons on the iron ions. These would contribute to the QS and to a $d|\epsilon|/dT < 0$.

The remaining chalcogenides $Fe_{1-x}M_2X_4$, $0 \leq x < 1$ and M = Ti, V, Zr, or Ta, may be considered layer compounds containing close-packed, metallic X–M–X layers with Fe^{2+} ions in octahedral interstices between the layers. Successive anion layers may be hexagonal close packed, as in the NiAs structure, or cubic close packed as in the CdI_2 structure. In the 2H–Ta_2S_4 structure, the M = tantalum atoms occupy trigonal prismatic sites rather than octahedral sites, which produces simple-hexagonal stacking of the anion within a layer X–M–X. In all these structures, the inserted iron atoms donate two electrons to the conducting sandwich, making them formally Fe^{2+} ions, and they experience an intrinsic trigonal field sensitive to the axial ratio c/a of the structure. The observed QS should reflect only the trigonal component of the crystalline field.

The low isomer shifts observed for FeV_2S_4 and V_3S_4 : Fe signal the possibility of low-spin iron; a low-spin Fe^{2+} state has been verified for V_5Se_8 : Fe (*62*).

The compounds $FePX_3$ and 1T–$Fe_{0.1}Ta_{0.9}S_2$ have no cations between layers. In the latter case, the iron appears to be in a low-spin state; in $FePX_3$ every three octahedral M atoms of the X–M–X layers are replaced by two Fe^{2+} ions and a P_2 molecular unit. The Fe^{2+} ions order into an hexagonal net having a P_2 unit at the center of each hexagon. This arrangement allows for Fe–Fe interactions that may delocalize the β-spin electrons, but the intrinsic trigonal field produces a QS. The IS is consistent with high-spin Fe^{2+} ions.

Of the remaining few compounds, the β-spin electrons are itinerant in cubanite **36**, $CuFe_2S_3$, and the low IS in the π phases with Co_9S_8 structure signal the presence of itinerant $3d$ electrons at low-spin iron

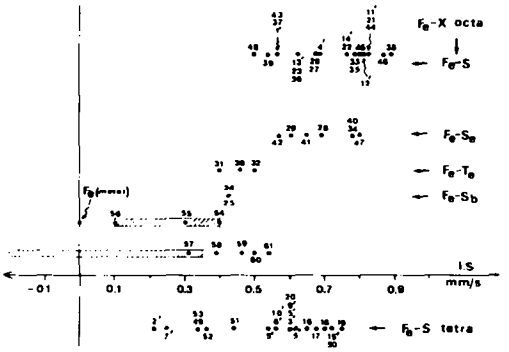

FIG. 1. Room-temperature isomer shifts relative to elemental iron for different Fe–X systems (X = S, Se, Te, Sb); see text. The IS refer to the metallic iron at 300 K, converted when necessary. Numbers refer to corresponding compounds listed in Table I. Simple numbers represent NiAs-type compounds, numbers marked with primes, spinel type.

atoms, consistent with the weak correlations manifest by a Pauli paramagnetism.

Figure 1 gives a graphical representation of the IS values of the compounds of Table I. The system corresponding to different anions X are shown separately. The numbers refer to the compound listing in Table I, the primed numbers marked with primes signaling the spinel structure. Numbers **54–61** refer, respectively, to the additional compounds Fe_5Sn_3, $Fe_{2-x}Ge$, Fe_5Si_3, the low-spin pyrite and marcassite phases FeS_2, $FeSe_2$, $FeTe_2$, and the compounds $Fe_{1/3}Ta_{2/3}S_2$ **60** and $Fe_{0.1}Ta_{0.9}Se_2$ **61**. All compounds falling in the cross-hatched region $0.1 \leq IS \leq 0.4$ mm/sec belong to intermetallic iron compounds (*47*) and those in the domain $-0.2 \leq IS \leq 0.35$ mm/sec to low-spin iron compounds. (*1*). Any spontaneous magnetism in the intermetallic compounds must be described by a strongly correlated band theory, not by a localized-electron crystal-field theory. Similarly, the tellurides, antimonides, π-phases, and vanadium layer compounds appear to contain itinerant Fe : $3d$ electrons with any spontaneous spin density at the iron atoms associated with holes in a low-spin Fe^{2+} : $t_2{}^6$ band. All these data are consistent with the formation of a low-spin state at iron atoms having an IS $\leq$ 0.5 mm/sec.

Conclusions

The "ferrous character" of the Mössbauer spectra of octahedral-site ^{57}Fe in iron chalcogenides and antimonides is principally due to an overlapping of the Fe^{2+} : $3d^6$ energies by the valence bands. However, with molar concentrations of holes in these bands, the Fermi energy E_F generally falls within a narrow band of Fe : $3d$ states to give a high density of states at E_F. In these cases, assignment of a formal valence to the iron atoms is meaningless.

Strong σ-bond covalent mixing makes the isomer shift small (IS < 0.9 mm/sec compared to an IS $\simeq$ 1.3–1.4 mm/sec in ferrous oxides and fluorides (*48, 49*)), and for an IS < 0.8 mm/sec the σ-bonding $3d$ electrons are probably itinerant σ^* electrons. However, the itinerant character of σ^* electrons at high-spin iron atoms is difficult to establish for Fe–X–M interac-

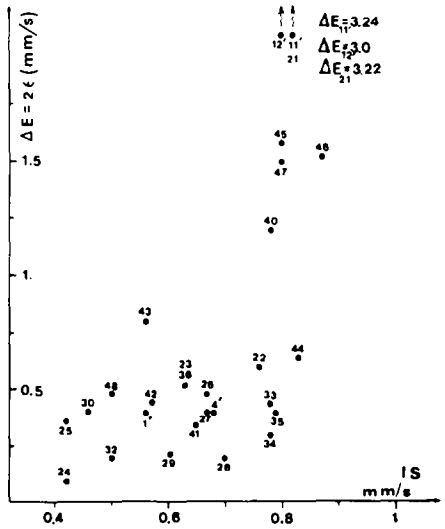

FIG. 2. Room-temperature quadrupole splitting $\Delta E_Q = 2\epsilon$ versus isomer shift (IS) for the octahedrally coordinated compounds.

tions, where M is a transition-metal atom other than iron. In the case of Fe–X–Fe interactions, spontaneous atomic moments due to σ^* electrons are sharply reduced from a localized-electron value in an antiferromagnetic state and the pressure dependence of the magnetic-ordering temperature is $dT_N/dP < 0$ (*3*).

For stronger covalent mixing, an IS < 0.5 mm/sec generally signals a low-spin state, and any spontaneous magnetism is only associated with holes in a low-spin Fe^{2+} t_2^6 band.

A localized d_β electron at high-spin Fe^{2+} ions can induce a QS in a cubic-field environment through a Jahn–Teller coupling to form vibronic states having accidental degeneracies lifted. The temperature dependence of such a QS is $d|\Delta E_Q|/dT < 0$. Where the QS is due to quadrupolar fields intrinsic to the crystal structure, any temperature dependence of the QS should follow the temperature dependence of the local deformation from cubic symmetry.

The magnitude of the QS associated with a time-averaged cubic field depends upon the Jahn–Teller splitting of vibronic states. This splitting decreases with increasing covalent mixing. Where important Fe–Fe interactions exist, the formation of itinerant β-spin electrons may eliminate any QS; but where the Fe–Fe interactions are negligible, a small QS may be associated with the formation of weakly coupled Jahn–Teller vibronic states.

Any linear IS/QS correlations should have limited applicability. Figure 2 shows the room-temperature QS $\Delta E_Q = 2\epsilon$ versus IS for the compounds of Table I. As in Fig. 1, the numbers indicate the corresponding compound in Table I. No linear IS/QS correlation is found among these iron compounds exhibiting "ferrous character."

References

1. N. N. GREENWOOD AND T. C. GIBB, *in* "Mössbauer Spectroscopy," p. 285, Chapman and Hall, London (1971).
2. F. VARRET, *J. Phys. (Paris)* **37**, C6-437 (1976).
3. J. B. GOODENOUGH, *Progr. Solid State Chem.* **5**, 145 (1972).
4. A. J. FREEMAN AND R. E. WATSON, *Phys. Rev.* **127**, 2058 (1962).
5. R. INGALLS, *Phys. Rev.* **133**, A787 (1964).
6. P. R. BRADY, J. F. DUNCAN, AND K. F. MOK, *Proc. Progr. Soc. A* **287**, 343 (1975).
7. T. C. GIBB AND N. N. GREENWOOD, *J. Chem. Soc.* **5**, 6989 (1965).
8. L. G. LANG, S. DE BENEDETTI, AND R. I. INGALLS, *J. Phys. Soc. Japan* **17**, Suppl. B-I, 131 (1962).
9. K. ONO, A. ITO, AND T. FUJITA, *J. Phys. Soc. Japan* **19**, 2119 (1964).
10. I. DEZSI AND L. KESZTHELYI, *Solid State Commun.* **5**, 511 (1966).
11. D. RAJ, K. CHANDRA, AND S. P. PURI, *J. Phys. Soc. Japan* **24**, 35 (1968).
12. S. CARIC, L. MARINKOV, AND J. SLIVKA, *Phys. Status Solidi A* **13**, 263 (1975).
13. J. R. SAMS AND T. BIK TSIN, *J. Chem. Phys.* **62**, 734 (1975).
14. W. NEUWIRTH AND H. J. SCHROTER, *Z. Phys. B* **23**, 71 (1976).
15. C. E. JOHNSON, *Proc. Phys. Soc.* **88**, 943 (1966).
16. J. F. CAVANACH, *Phys. Status Solidi* **36**, 657 (1969).
17. M. G. CLARK, G. M. BANCROFT, AND A. J. STONE, *J. Chem. Phys.* **17**, 4250 (1967).
18. P. IMBERT AND E. MARTEL, *C.R. Acad. Sci. Paris* **261**, 5404 (1965).
19. P. IMBERT, *C.R. Acad. Sci. Paris* **263**, 767 (196).
20. F. HARTMANN-BOUTRON AND P. IMBERT, *J. Appl. Phys.* **39**, 775 (1968).
21. F. VARRET AND P. IMBERT, *J. Phys. Chem. Solids* **35**, 215 (1974).
22. M. EIBSCHUTZ, U. GANIEL, AND S. SHTRIKMAN, *Phys. Rev.* **151**, 245 (1966).
23. M. EIBSCHUTZ AND U. GANIEL, *Solid State Commun.* **5**, 267 (1967).
24. M. EIBSCHUTZ, U. GANIEL, AND SHTRIKMAN, *Phys. Rev.* **156**, 259 (1967).
25. C. BLAAUW, F. LEENHOUTS, AND F. VAN DER WOUDE, *J. Phys. (Paris)* **37**, C6-607 (1976).
26. M. EIBSCHUTZ, E. HERMON, AND S. SHTRIKMAN, *J. Phys. Chem. Solids* **28**, 1633 (1967).
27. L. M. BELYAEV, T. V. DIMITRIEVA, I. S. LYUBUTIN, A. P. MAZAHARA, AND V. E. FEDOROV, *Sov. Phys. JETP* **41**, 583 (1975).
28. L. BROSSARD, H. OUDET, AND P. GIBART, *J. Phys. (Paris)* **37**, C6-23 (1976).
29. A. GERARD, P. IMBERT, H. PRANGE, F. VARRET,

AND M. WINTENBERGER, *J. Phys. Chem. Solids* **32,** 2091 (1971).
30. H. J. VAN BARDELEBEN, A. L. GOLTZENE, AND C. SCHWABB, *J. Appl. Phys.* **46,** 1736 (1975).
31. M. EIBSCHUTZ, E. HERMON, AND S. SHTRIKMAN, *Solid State Commun.* **5,** 529 (1967).
32. Y. HAZONY, *in* "Mössbauer Effect Methodology" (I. J. Cruvezman, Ed.), Vol. 7, p. 153, Plenum, New York (1971).
33. Y. HAZONY, *Phys. Rev. B* **3,** 711 (1971).
34. R. GARG AND V. K. GARG, *Phys. Status Solidi B* **77,** K165 (1976).
35. K. MIZUSHIMA, M. TANAKA, A. ASCI, S. IDA, AND J. B. GOODENOUGH, *J. Phys. Chem. Solids,* in press.
36. J. B. GOODENOUGH, *Mater. Res. Bull.* **13,** 1305 (1978).
37. A. M. VAN DIEPEN AND R. P. VAN STAPELE, *Solid State Commun.* **13,** 1651 (1973).
38. M. R. SPENDER AND A. H. MORRISH, *Canad. J. Phys.* **50,** 1125 91972); *Solid State Commun.* **11,** 1417 (1972).
39. F. K. LOTGERING, *Philips Res. Rep.* **11,** 190 (1956).
40. M. R. SPENDER, J. M. D. COY, AND A. H. MORRISH, *Canad. J. Phys.* **50,** 2313 (1972).
41. G. A. FATSEAS, J. L. DORMANN, AND H. OUDET, *in* "Proceedings, International Conference on Mössbauer Spectroscopy, Bucharest, September 1977" (D. Barb and D. Tarina, Eds.), p. 175.
42. G. A. FATSEAS, J. L. DORMANN, R. DRUILHE, L. BROSSARD, AND P. GIBART, *Physica* **86-88B,** 887 (1977).
43. G. A. FATSEAS, M. DANOT, AND J. L. DORMANN, to be published.
44. M. KAWAMINAMI AND A. OKAZAKI, *J. Phys. Soc. Japan* **29,** 649 (1970).
45. J. SERRE, P. GIBART, AND J. BONNEROT, *J. Phys. (Paris)* **30,** 93 (1969); J. FRIEDEL, G. LEMAN, AND S. OLSZEWSKI, *J. Appl. Phys.* **32,** 3255 (1961).
46. K. OZAWA, T. YOSHIMI, S. ANZAI, AND S. YANAGISAMA, *Phys. Status Solidi A* **19,** K39 (1973).
47. G. A. FATSEAS, *Phys. Rev. B* **8,** 43 (1973).
48. L. R. WALKER, G. K. WERTHEIM, AND V. JACCARINO, *Phys. Rev. Lett.* **6,** 98 (1961).
49. J. DANON, *Tech. Rep. Ser. IAEA* **50,** 89 (1966).
50. P. GIBART, L. GOLDSTEIN, AND L. BROSSARD, *J. Magn. Mater.* **3,** 109 (1976).
51. M. TANAKA, T. TOKORO, AND T. MORI, *in* "Proceedings, International Conference on Mössbauer Spectroscopy, Bratislava, 1973" (Czechoslovak Atomic Energy Commission, Eds.), Praha 5 Zbrasla (1975).
52. M. R. SPENDER AND A. H. MORRISH, *Solid State Commun.* **11,** 1417 (1972).
53. L. BROSSARD, L. GOLDSTEIN, AND M. GUITTARD, *J. Phys. (Paris)* **37,** C6-493 (1976).
54. A. AHOUANDJINOU, "Les systèmes formés entre le fer, le cobalt, le nickel et les diséléniures de titane et de zirconium," Thèse d'Etat, UER de Chimie, Université de Nantes, France, 13 July 1977.
55. J. R. GOSSELIN, M. G. TOWSEND, R. J. TREMBLAY, AND A. H. WEBSTER, *Mater. Res. Bull.* **10,** 41 (1975).
56. L. M. LEVINSON AND D. TREVES, *J. Phys. Chem. Solids* **29,** 2227 (1968).
57. G. N. GONCHAROV, YU. M. OSTANEVICH, S. B. T. MILOV, AND L. CSER, *Phys. Status Solidi* **37,** 141 (1970).
58. C. BOUMFORD AND A. H. MORRISH, *Phys. Status Solidi A* **22,** 435 (1974).
59. H. NAM OK AND S. WON LEE, *Phys. Rev. B* **8,** 4267 (1973).
60. S. MURANAKA, *J. Phys. Soc. Japan* **35,** 1553 (1973).
61. G. A. FATSEAS, J. L. DORMANN, AND M. DANOT, *J. Phys. (Paris)* **37,** C6-79 (1976).
62. Y. OKA, K. KOSUGE, AND S. KACHI, *Mater. Res. Bull.* **12,** 1117 (1977).
63. S. R. HONG AND H. NAM OK, *Phys. Rev. B* **11,** 4176 (1975).
64. M. EIBSCHUTZ, F. J. DI SALVO, G. W. HULL, JR., AND S. MAHAJAN, *Appl. Phys. Lett.* **27,** 464 (1975).
65. J. CHAPPERT AND G. A. FATSEAS, *C.R. Acad. Sci. Paris Ser. B* **262,** 242 (1966).
66. P. MANCA, J. P. SUCHET, AND G. A. FATSEAS, *Ann. Phys. (Paris)* **1,** 621 (1966).
67. V. FANO AND I. ORTALLI, *Phys. Status Solidi A* **10,** K121 (1972).
68. K. V. REDDY AND S. C. CHETTY, *Phys. Status Solidi A* **37,** 687 (1976).
69. J. SUCHET AND P. IMBERT, *C.R. Acad. Sci. Paris* **260** (groupe 6), 5239 (1965).
70. K. YAMAGUCHI, H. YAMOMOTO, Y. HAMAGUCHI, AND H. WATANABE, *J. Phys. Soc. Japan* **33,** 1292 (1972).
71. F. W. RICHTER AND K. SCHMIDT, *Z. Naturforsch. A* **30,** 1621 (1975).
72. K. B. LAL, S. MENDIRATA, AND G. N. RAO, *Phys. Status Solidi A* **32,** K79 (1975).
73. M. ABE, K. KANETA, AND K. UCHINO, *J. Phys. Soc. Japan* **44,** 1739 (1978).
74. B. E. TAYLOR, J. STEGER, AND A. WOLD, *J. Solid State Chem.* **7,** 461 (1973).
75. B. TAYLOR, J. STEGER, A. WOLD, AND E. KOSTINER, *Inorg. Chem.* **13,** 2719 (1974).

76. H. HORITA AND E. HIRAHARA, *Sci. Rep. Tohoku Univ. Ser. I* **54**, No. 3, 127 (1971).
77. J. R. REGNARD AND J. C. HOCQUE NGHEM, *J. Phys. (Paris)* **32**, C1-268 (1971).
78. C. MEYER, Y. GROS, H. VINCENT, AND E. F. BERTAUT, *J. Phys. Chem. Solids* **37**, 1153 (1976).
79. G. HAACKE AND L. C. BEEGLE, *J. Phys. Chem. Solids* **28**, 1699 (1967).
80. E. F. BERTAUT, *Bull. Soc. Fr. Mineral. Cristallogr.* **79**, 276 (1956).
81. S. ANZAI AND K. OZAWA, *Phys. Status Solidi A* **24**, K31 (1974).
82. J. M. D. COEY, H. ROUX BUISSON, AND A. CHAMBEROD, *Solid State Commun.* **13**, 43 (1973).
83. I. G. KERIMOV, A. M. MUSAYEV, M. M. KURBANOV, D. A. GUSEYNOV, AND R. Z. SADYKHOV, *Fiz. Metal. Metalloved.* **37**, 1101 (1974).
84. S. MURANAKA AND T. TAKADA, *Bull. Inst. Chem. Res. Kyoto Univ.* **51**, 287 (1973).
85. D. BABOT, G. BERODIAS, AND B. LAMBERT-ANDRON, *J. Phys. (Paris)* **32**, C1-985 (1971).
86. L. GOLDSTEIN, L. BROSSARD, M. GUITTARD, AND J. L. DORMANN, *in* "Proceedings, International Conference on Magnetism," p. 889, North-Holland, Amsterdam (1976).
87. T. TAKAHASHI AND O. YAMADA, *J. Solid State Chem.* **7**, 25 (1973).
88. T. YASHIRO, Y. YAMAGUCHI, S. TOMIYOSHI, N. KAZAMA, AND H. WATANABE, *J. Phys. Soc. Japan* **34**, 58 (1973).
89. K. ADACHI, *J. Phys. Soc. Japan* **16**, 2187 (1961).
90. L. TRICHET, J. ROUXEL, AND M. M. POUCHARD, *J. Solid State Chem.* **14**, 283 (1975).
91. M. DANOT, J. ROUXEL, AND O. GOROCHOV, *Mater. Res. Bull.* **9**, 1383 (1974).
92. J. SUCHET AND J. SERRE, *C.R. Acad. Sci. Paris* **260**, 3890 (1965).
93. F. K. LOTGERING, A. M. VAN DIEPEN, AND J. F. OLIJHOEK, *Solid State Commun.* **17**, 1149 (1975).
94. M. EIBSCHUTZ AND F. J. DI SALVO, *Phys. Rev. Lett.* **36**, 104 (1976).
95. O. KNOP, C. H. HUANG, K. I. G. REID, J. S. CARLOW, AND F. W. D. WOODHAMS, *J. Solid State Chem.* **16**, 97 (1976).
96. E. F. BERTAUT, P. BURLET, AND J. CHAPPERT, *Solid State Commun.* **3**, 335 (1965).
97. A. GERARD, P. IMBERT, H. PRANGE, F. VARRET, AND M. WINTENBERGER, *J. Phys. Chem. Solids* **32**, 2091 (1971).
98. G. GARCIN, P. IMBERT, AND G. JEHANO, *Solid State Commun.* **21**, 545 (1977).
99. G. HAACKE AND A J. NOJIK, *Solid State Commun.* **6**, 363 (1968).
100. L. M. BELYAEV, T. V. DIMITRIEVA, I. S. LYUBUTIN, A. P. MAZHARA, AND V. E. FEDOROV, *Sov. Phys. JETP* **41**, 583 (1976).
101. L. BROSSARD, H. OUDET, AND P. GIBART, *J. Phys. (Paris)* **37**, C6-23 (1976).
102. F. K. LOTGERING, A. M. VAN DIEPEN, AND J. F. OLIJHOEK, *Solid State Commun.* **17**, 1149 (1975).
103. M. R. SPENDER AND A. H. MORRISH, *in* "Proceedings, 5th International Conference on Mössbauer Spectroscopy, Bratislava, September 1973" (Czechoslovak Atomic Energy Commission, Eds.), Vol. 1, p. 125, Praha 5 Zbraslav (1975).
104. A. M. VAN DIEPEN AND R. P. VAN STAPELE, *Phys. Rev. B* **5**, 2467 (1972).
105. H. KONDO, *J. Phys. Soc. Japan* **41**, 1247 (1976).
106. F. K. LOTGERING, *J. Phys. (Paris)* **32**, C1-34 (1971).
107. M. EIBSCHUTZ, E. HERMON, AND S. SHTRIKMAN, *J. Phys. Chem. Solids* **28**, 1633 (1967).
108. H. J. VON VARDELEBEN, A. GOLTZENE, AND C. SCHWAB, *J. Appl. Phys.* **46**, 1736 (1975).
109. J. ACKERMANN, S. SOLED, A. WOLD, AND E. KOSTINER, *J. Solid State Chem.* **19**, 75 (1976).
110. N. N. GREENWOOD AND H. J. WHITFIELD, *Inorg. Phys. Theor. J. Chem. Soc. A*, 1697 (1968).
111. C. B. VAN DER BERG AND R. THIEL, *Z. Anorg. Allg. Chem.* **106**, 368 (1969).
112. R. C. THIEL, *Phys. Status Solidi* **40**, K17 (1970).
113. P. GIBART, J. L. DORMANN, AND Y. PELLERIN, *Phys. Status Solidi* **36**, 187 (1969).
114. M. R. SPENDER AND A. H. MORRISH, *Canad. J. Phys.* **49**, 2659 (1971).
115. R. P. VAN STAPELE, J. S. VAN WIERINGEN, AND P. F. BONGERS, *J. Phys. (Paris)* **32**, C1-53 (1971).
116. J. L. HORWOOD, M. G. TOWSEND, AND A. H. WEBSTER, *J. Solid State Chem.* **17**, 35 (1976).
117. R. GOSSELIN, M. G. TOWSEND, R. J. TREMBLAY, AND A. H. WEBSTER, *J. Solid State Chem.* **17**, 43 (1976).
118. A. OKAZAKI, *J. Phys. Soc. Japan* **16**, 1162 (1961).
119. J. E. GOODENOUGH, *Solid State Commun.* **5**, 577 (1967).
120. C. CHIRANE, R. E. COX, AND S. J. PICKART, *J. Appl. Phys.* **35**, 954 (1964).
121. P. K. BALTZER, P. J. WOJTOWICZ, M. ROBBINS, AND E. LOPATIN, *Phys. Rev.* **151**, 367 (1966).
122. M. EIBSCHUTZ AND F. J. DI SALVO, *Phys. Rev. B* **15**, 5181 (1977).